Frontiers of Information Technology & Electronic Engineering
www.jzus.zju.edu.cn; engineering.cae.cn; www.springerlink.com
ISSN 2095-9184 (print); ISSN 2095-9230 (online)
E-mail: jzus@zju.edu.cn

Correction of array failure using grey wolf optimizer hybridized with an interior point algorithm*

Shafqat Ullah KHAN†[1], M. K. A. RAHIM[1], Liaqat ALI[2]

[1]*Advanced RF & Microwave Research Group, Department of Communication Engineering, Faculty of Electrical Engineering, Universiti Teknologi Malaysia, Skudai 81310, Malaysia*

[2]*Department of Electrical Engineering, University of Science and Technology Bannu, Bannu 28100, Pakistan*

†E–mail: shafqatphy@yahoo.com

Received Nov. 14, 2016; Revision accepted Feb. 21, 2017; Crosschecked Sept. 17, 2018

Abstract: We design a grey wolf optimizer hybridized with an interior point algorithm to correct a faulty antenna array. If a single sensor fails, the radiation power pattern of the entire array is disturbed in terms of sidelobe level (SLL) and null depth level (NDL), and nulls are damaged and shifted from their original locations. All these issues can be solved by designing a new fitness function to reduce the error between the preferred and expected radiation power patterns and the null limitations. The hybrid algorithm has been designed to control the array's faulty radiation power pattern. Antenna arrays composed of 21 sensors are used in an example simulation scenario. The MATLAB simulation results confirm the good performance of the proposed method, compared with the existing methods in terms of SLL and NDL.

Key words: Failure correction; Grey wolf optimizer; Interior point algorithm; Sidelobes; Deeper null depth level
https://doi.org/10.1631/FITEE.1601694 **CLC number:** TN929

1 Introduction

Detection and correction of faulty arrays in beamforming are practical issues. In satellite and radar communication systems, an array antenna is of great importance in achieving adaptive beamforming (Ram et al., 2017). The demand for large antenna arrays grows day by day due to their low cost and good null, and main beam-steering abilities. Because these arrays are large, there is always a chance of failure of a single or multiple sensors. The failure of sensors can damage the entire radiation power pattern in terms of the sidelobe level (SLL) and null depth level (NDL), move nulls from their original locations, and increase the main beam width. Thus, sensor failure can affect the entire pattern, and communication becomes impossible. The replacement of faulty sensors in satellite communications is not possible, presenting a big challenge for researchers to continue the desired communications.

Diagnosis and recovery of faults in antenna arrays have received much attention in recent years. Once the location of the faulty sensors is detected using fault detection techniques (Choudhury et al., 2013; Fonollosa et al., 2013; Khan et al., 2015a, 2016a, 2016b, 2017; Zhu et al., 2015), correction techniques are applied to recover the desired pattern (Peters, 1991; Hejres et al., 2007; Acharya et al., 2014; Hejres, 2004; Khan et al., 2014, 2015b, 2015c; Poli et al., 2014). Zhu et al. (2015) developed an algorithm to diagnose a faulty antenna array that does not require a priori knowledge of the faulty elements. A number of techniques are available in the literature to correct the

* Project supported by the Ministry of Higher Education (MOHE), the Research Management Centre (RMC), the School of Postgraduate Studies (SPS), the Communication Engineering Department, the Faculty of Electrical Engineering (FKE), and Universiti Teknologi Malaysia (UTM) Johor Bahru (Nos. 12H09 and 03E20tan)

ORCID: Shafqat Ullah KHAN, http://orcid.org/0000-0003-1969-1289

damaged radiation power pattern by adjusting the weights of the remaining sensors.

In recent years, some conventional methods have been used to correct the faulty pattern by adjusting the weights of active sensors in the array using nature-inspired optimization techniques to achieve the desired pattern (Acharya et al., 2011; Khan et al., 2015b). Peters (1991) proposed a conjugate gradient technique to reconfigure the weights and phase distribution of active sensors in the array by decreasing only the average SLL. Poli et al. (2014) proposed a technique based on a time-modulated array (TMA) to correct array failures. In the correction of faulty arrays, with a reduction in SLL, null and beam steerings become important issues to be addressed. Compensation has been presented to sustain fixed nulls and null steering in phased antenna arrays (Hejres, 2004; Hejres et al., 2007). Yeo and Lu (1999) proposed a genetic algorithm, which reduces only SLL, to correct failures. Acharya et al. (2014) proposed a method to compensate for the failure in faulty arrays. The first part of their study deals with thinning in the faulty arrays (i.e., finding the minimum number of working sensors of the array that can recover the desired pattern), while the second part deals with the maximum number of faulty elements that can be compensated for using particle swarm optimization, but this method reduces only SLL. The symmetrical linear array is of great importance and has already shown useful results in achieving the desired pattern (Khan et al., 2013). A linear symmetrical array antenna is used to correct failures, where the failed element signals are reconstructed from the failed elements by taking their conjugates (Khan et al., 2016c).

With a growing interest in application, nature-inspired evolutionary computational techniques have been doing well in solving numerous search and optimization problems due to the impartial nature of their operations, which can still be useful in situations without domain knowledge (Shoaib et al., 2015; Zou et al., 2016; Raja et al., 2017; Zhang et al., 2017). The search method using evolutionary algorithms (EAs) is impartial, and there is no domain knowledge to guide the search method. Domain knowledge assists as a method to decrease the search space by thinning unnecessary parts of the solution space and by promoting required parts. The grey wolf (*Canis lupis*) belongs to the *Canidae* family and is the inspiration for the grey wolf optimizer (GWO), a latest nature-inspired global search algorithm (Mirjalili et al., 2014). GWO is hybridized with the local search optimization technique for the best results.

In this paper, the proposed technique resolves the issues of faulty patterns in terms of reduced SLL, deeper NDL, and dislocation of nulls from their original locations better than the available techniques. We design a new fitness function and GWO along with an interior point algorithm (IPA) to achieve a reduced SLL, a deeper NDL, and restoration of nulls to their original locations by adjusting the current weights of active sensors in the array. Moreover, proper settings of parameters used in the fitness function have a deeper effect on the radiation power pattern. A hybrid method based on the memetic computing algorithm is proposed, which combines GWO with IPA for the reduction of SLL and the deepening of NDL. Various simulation results are provided to confirm the performance of the proposed technique, which is compared with those of the available techniques.

2 Problem formulation

Consider an array of linear antennas composed of 21 sensors positioned symmetrically about the origin. The total number of sensors is $N=2K+1$, where K is the number of sensors on either side of the array center. The array factor in this healthy setup with equally spaced sensors, nonuniform weights, and progressive phase excitation was proposed by Wolff (1937), as follows:

$$\mathrm{AF}(\theta_i)=\sum_{n=-K}^{K} w_n \exp\left(\mathrm{j}n(kd\cos\theta_i+\gamma)\right), \qquad (1)$$

where θ_i (i=1, 2, …, M_0) is the interfering angle, w_n is the weight of the antenna sensor (n=0, ±1, ±2,… , ±K), d is the distance between the antenna sensors, θ is the angle from broadside, $k=2\pi/\lambda$ is the wave number where λ is the wavelength, and $\gamma=-kd\cos\theta_s$ is the phase shift where θ_s is the main beam-directing angle. Now if some sensors in the array fail, the array factor for the damaged power pattern can be given as

$$\mathrm{AF}(\theta_i)=\sum_{\substack{n=-K\\ n\neq 2,5}}^{K} w_n \exp\left(\mathrm{j}n(kd\cos\theta_i+\beta)\right), \tag{2}$$

where β is used to control the nulls at a particular angle.

It is assumed that sensors w_2 and w_5 fail in the array antenna. One can obviously see from Fig. 1 that due to the damage to sensors w_2 and w_5, the power pattern is impaired in terms of SLL, NDL, diminishing of nulls, and dislocation of the nulls from their original locations.

Thus, the objective of this study is to recover a deeper NDL, reduce SLL, and restore the nulls to their original locations. In the literature, several methods are available to correct the faulty pattern; however, none of them is able to achieve the required SLL and deeper NDL in the direction of the interferer.

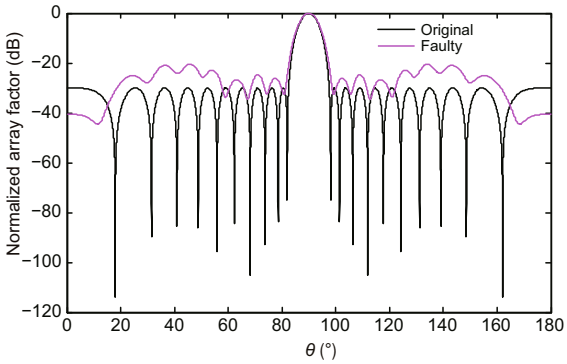

Fig. 1 Original and faulty (w_2, w_5) radiation power patterns (References to color refer to the online version of this figure)

3 The proposed solution for array failure correction

In this section, we develop the proposed solution based on the design of a new fitness function. Because we assume that sensors w_2 and w_5 are damaged, we lose the NDL, and experience diminished nulls, movement of nulls from their original locations, and an SLL (Fig. 1). By designing a new fitness function, we achieve deeper NDL and SLL using GWO and IPA.

3.1 Grey wolf optimizer (GWO)

GWO is the latest nature-motivated global search algorithm. In GWO, the heads are a male and a female, called 'alphas'. The alpha is accountable for making decisions about hunting and sleeping places. The alphas' decisions are verbalized to the container. In GWO, the alpha wolf is called the 'dominant wolf' (Mirjalili et al., 2014). Interestingly, the alpha is not necessarily the strongest candidate of the container, but it is the best in terms of managing the container. The second level of GWO is the beta. These betas help the alpha in decision-making and respect the alpha wolves. Omegas are lower-ranking grey wolves and are the last wolves that are permitted to eat. If a wolf is not an alpha, beta, or omega, it is called a 'delta wolf'. Delta wolves are of lower rank than the alpha and betas, but they lead the omegas. This arrangement has a number of applications in the field of science and engineering (Muro et al., 2011; Uysal and Bayir, 2013; Song et al., 2014; Wong et al., 2014; El-Gaafary et al., 2015). Mirjalili et al. (2014) gave the basic steps of GWO as follows:

1. tracing, hunting, and finding the prey;
2. chasing, encircling, and harassing the prey until it stops moving;
3. attacking toward the prey.

The surrounding behavior is modeled mathematically by (Mirjalili et al., 2014)

$$\begin{cases} \boldsymbol{D}=\left|\boldsymbol{C}\cdot\boldsymbol{w}_{\mathrm{P}}(t)-\boldsymbol{w}(t)\right|, \\ \boldsymbol{w}(t+1)=\boldsymbol{w}_{\mathrm{P}}(t)-\boldsymbol{A}(\boldsymbol{D}), \end{cases} \tag{3}$$

where t is the current iteration, $\boldsymbol{A}$ and $\boldsymbol{C}$ are the coefficient vectors, $\boldsymbol{w}_{\mathrm{P}}$ is the position vector of the prey, $\boldsymbol{w}$ is the position vector of the grey wolf, and $\boldsymbol{D}$ represents the modified weights. Vectors $\boldsymbol{A}$ and $\boldsymbol{C}$ are calculated as follows:

$$\begin{cases} \boldsymbol{A}=2\boldsymbol{a}\cdot\boldsymbol{r}_1-\boldsymbol{a}, \\ \boldsymbol{C}=2\boldsymbol{r}_2, \end{cases} \tag{4}$$

where the components of $\boldsymbol{a}$ are linearly decreased from 2 to 0, and $\boldsymbol{r}_1$ and $\boldsymbol{r}_2$ are random vectors whose modules are in range [0, 1]. The optimization process is guided by α, β, and δ, while ω wolves follow these three kinds of wolves. The three kinds of wolves (α, β, and δ) are supposed to have superior knowledge about the location of the prey. Therefore, the three best solutions are kept and the other agents update their locations to the location of the best search agent. For this purpose, we use

$$\begin{cases} \boldsymbol{D}_\alpha = \left|\boldsymbol{C}_1 \cdot \boldsymbol{w}_\alpha - \boldsymbol{w}\right|, \\ \boldsymbol{D}_\beta = \left|\boldsymbol{C}_2 \cdot \boldsymbol{w}_\beta - \boldsymbol{w}\right|, \\ \boldsymbol{D}_\delta = \left|\boldsymbol{C}_3 \cdot \boldsymbol{w}_\delta - \boldsymbol{w}\right|, \end{cases} \tag{5}$$

$$\begin{cases} \boldsymbol{w}_1 = \left|\boldsymbol{w}_\alpha - \boldsymbol{A}_1 \boldsymbol{D}_\alpha\right|, \\ \boldsymbol{w}_2 = \left|\boldsymbol{w}_\beta - \boldsymbol{A}_2 \boldsymbol{D}_\beta\right|, \\ \boldsymbol{w}_3 = \left|\boldsymbol{w}_\delta - \boldsymbol{A}_3 \boldsymbol{D}_\delta\right|, \end{cases} \tag{6}$$

$$\boldsymbol{w}(t+1) = \frac{1}{3}(\boldsymbol{w}_1 + \boldsymbol{w}_2 + \boldsymbol{w}_3). \tag{7}$$

Using Eq. (6), an agent updates its location according to α, β, and δ. Therefore, α, β, and δ evaluate the location of the prey, and the other wolves distribute their locations randomly around the prey. The basic steps of GWO are as follows:

1. Generate a random population of grey wolves.

2. α, β, and δ wolves evaluate the possible locations of the prey over the iteration. Each possible solution establishes its distance from the prey.

3. Factor $|\boldsymbol{a}|$ is decreased from 2 to 0 to stress searching (exploration) and attacking (exploitation) the prey. The possible solutions converge to the prey when $|\boldsymbol{A}|>1$ and diverge when $|\boldsymbol{A}|<1$; when $|\boldsymbol{A}|=1$, we will not converge to the desired result.

4. Finally, GWO is terminated if the desired fitness is achieved.

3.2 Interior point algorithm (IPA)

IPA is a local search technique for fine tuning the antenna weights. This is a derivative-based algorithm derived from Lagrange multipliers (Wright, 1997; Potra and Wright, 2000). In IPA, some parameters, such as the number of maximum perturbations, the types of derivative and scaling function, are involved, while the setting involves boundaries based on the upper and lower limits, fitness limit, Hessian function, nonlinear constraint tolerance, and minimum perturbation. The parameters used are given in Table 1.

3.3 Hybrid algorithm: grey wolf optimizer-interior point algorithm (GWO-IPA)

Once we have achieved results with the global search optimizer, a local search is used for fine tuning. The results obtained by the global search optimizer are good to the estimated solution; however, the accuracy level is low, whereas the local search algorithm has an excellent estimated time complexity but gets stuck at the local minima. However, the hybrid algorithm uses the abilities of the global search optimizer and the local search algorithm to obtain the desired results. The flow diagram of the hybridized GWO-IPA is shown in Fig. 2.

Table 1 Settings of parameters for the interior point algorithm

Parameter	Setting
Maximum perturbation	0.2
Minimum perturbation	10^{-5}
Scaling	Constraint and objective
Sub-problem algorithm	IDI factorization
Hessian	BFGS
Type of derivative	Central difference
Penalty factor	50
Maximum number of function evaluations	1000
Maximum number of iterations	500
Fitness limit	10^{-10}

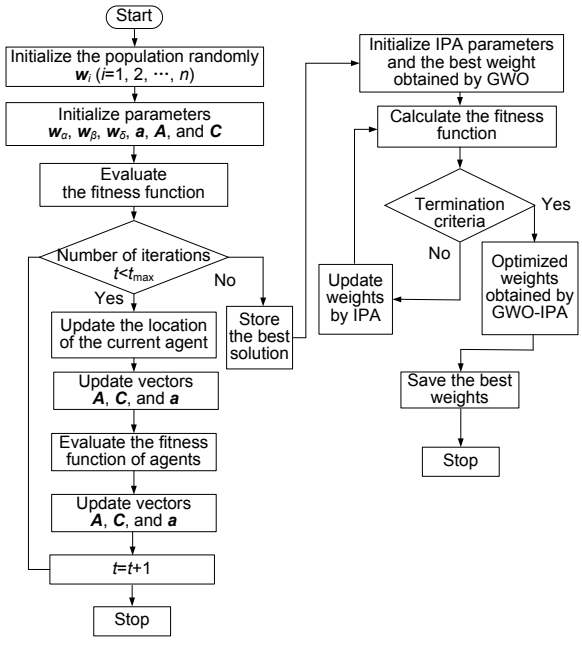

Fig. 2 Flowchart of the hybridized GWO-IPA
GWO: grey wolf optimizer; IPA: interior point algorithm

3.4 Null limitation (NL)

In mobile and radar communication systems, we want to avoid interfering signals positioned at the precise angle. For these applications, to put a null at the interfering angle θ_i, the null limitation (NL) is given by

$$\mathrm{AF}(\theta_i)=\boldsymbol{w}^{\mathrm{H}}\boldsymbol{a}(\theta_i)=0, \tag{8}$$

where $\boldsymbol{a}(\theta_i)$ and $\boldsymbol{w}^{\mathrm{H}}$ are $N\times1$ vectors with the following pattern:

$$\boldsymbol{a}(\theta_i)=\begin{bmatrix}\exp\left(-\mathrm{j}\dfrac{N-1}{2}kd\cos\theta_i\right)\\ \exp\left(-\mathrm{j}\dfrac{N-3}{2}kd\cos\theta_i\right)\\ \vdots\\ \exp(0)\\ \vdots\\ \exp\left(\mathrm{j}\dfrac{N-3}{2}kd\cos\theta_i\right)\\ \exp\left(\mathrm{j}\dfrac{N-1}{2}kd\cos\theta_i\right)\end{bmatrix}_{N\times1}, \tag{9}$$

$$\boldsymbol{w}=\left[w_{-M},w_{-M+1},\cdots,w_0,\cdots,w_{M-1},w_M\right]^{\mathrm{T}}. \tag{10}$$

The null limitation is set as

$$\boldsymbol{w}^{\mathrm{H}}\boldsymbol{a}(\theta_i)=0,\ i=1,2,....M_0. \tag{11}$$

By defining an $N\times M_0$ constraint matrix, we have

$$\boldsymbol{C}=\left[\boldsymbol{a}(\theta_1),\boldsymbol{a}(\theta_2),\cdots,\boldsymbol{a}(\theta_{M_0})\right], \tag{12}$$

where M_0 is the null direction. Our goal is to improve the squared weighting error subject to

$$\boldsymbol{w}^{\mathrm{H}}\boldsymbol{C}=0. \tag{13}$$

Our restriction is that the columns of $\boldsymbol{C}$ should be orthogonal to weight vector $\boldsymbol{w}$. Therefore, we may define G_i (i=1, 2, 3) and G as

$$G_1=\left|\mathrm{AF}_d(\theta_{\mathrm{maxSLL}},w_n)\right|/\left|\mathrm{AF}_{\mathrm{GWO}}(\theta_0,w_n)\right|, \tag{14}$$

$$G_2=\left\|\boldsymbol{w}^{\mathrm{H}}\boldsymbol{C}\right\|^2, \tag{15}$$

$$G_3=(w_{\pm n})_{\mathrm{SEF}}, \tag{16}$$

$$G=G_1+G_2+G_3.$$

The following fitness function is used to decrease SLL, deepen NDL, and restore the nulls to their desired locations in the track of interferers:

$$\begin{aligned}\text{Cost function}=&\alpha\left|\mathrm{AF}_d(\theta_{\mathrm{maxSLL}},w_n)\right|/\left|\mathrm{AF}_{\mathrm{GWO}}(\theta_0,w_n)\right|\\&+\beta\|\boldsymbol{w}^{\mathrm{H}}\boldsymbol{C}\|^2+\gamma(w_{\pm n})_{\mathrm{SEF}},\end{aligned} \tag{17}$$

where θ_{maxSLL} indicates the maximum SLL, θ_0 represents the maximum radiation pattern angle in the range of [0, π], $\mathrm{AF}_{\mathrm{GWO}}(\theta_0, w_n)$ is the array factor optimized by GWO, $(w_{\pm n})_{\mathrm{SEF}}$ is the symmetrical element failure weight of the n^{th} sensor, α is the weighting factor used to control SLL, β is the factor used to control the nulls at a particular angle, and γ is used to control NDL. Eq. (17) consists of three factors, which are necessary for the failure correction problem.

Hence, this is the fitness function for optimization of the given problem discussed above. The finest chromosome will give the smallest value of the fitness function. The first term in Eq. (17) is used to reduce SLL, where $\mathrm{AF}_d(\theta_i)$ denotes the preferred pattern and $\mathrm{AF}_{\mathrm{GWO}}(\theta_i)$ is the pattern obtained by GWO. The second term in Eq. (17) is used to suppress and restore the nulls to their previous locations after sensor failure. The third term is used to produce a deeper NDL.

4 Results and discussion

In this section, the simulation results obtained using the proposed and conventional techniques are presented for a Dolph-Chebyshev array of 21 sensors with a fixed intersensor spacing of $\lambda/2$. We used a constant radiation power pattern of SLL with −30 dB as a reference array with nulls at the particular directions. The results are shown for different numbers of nulls recovery, reduction of SLL, and main beam steering scenario, and are then compared with those of conventional techniques.

4.1 Results of the proposed method

In this case, we assumed that sensors w_2 and w_5 were damaged completely. Consequently, the entire radiation power pattern was disturbed, mainly in terms of SLL and NDL, and the nulls were displaced from their original locations. To nearly restore the original pattern, we designed a new fitness function using GWO along with an IPA to reduce SLL and NDL, and restore the nulls to their original locations. Due to the sensor (w_2 and w_5) failures, SLL increased to −23.06 dB (Fig. 3). The SLL and NDL for the damaged array were obtained using the proposed technique, as shown in Table 2. The recovery of one null using the proposed technique is given in Fig. 3.

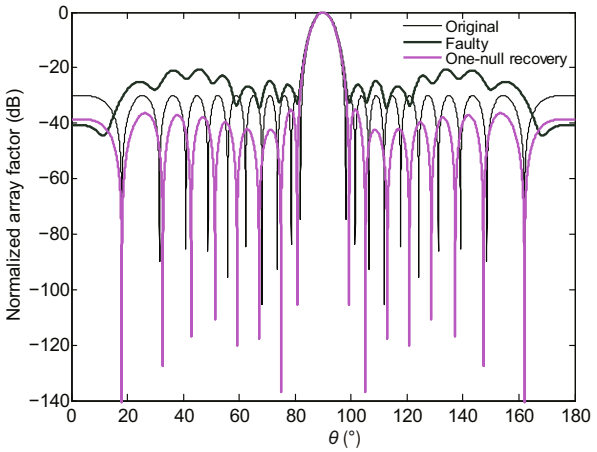

Fig. 3 The original, faulty, and one-null recovered radiation power patterns (References to color refer to the online version of this figure)

Table 2 Comparison of SLL and NDL in the original, faulty, and one-null recovered radiation power patterns

Pattern	Array factor (dB)	
	SLL	NDL
Original	−30.00	−140.00
Damaged	−23.06	−44.13
Recovered	−38.57	−140.00

SLL: sidelobe level; NDL: null depth level

After applying the proposed technique, SLL was reduced to −38.57 dB. Thus, the proposed method achieved a −15 dB SLL reduction and a −96 dB deeper null restored to their original locations.

If two interferers were coming from two different directions, then our desire was to put minimum energy in those directions, i.e., to put a null in the desired directions. Fig. 4 depicts the recovery of two nulls with the reduction of SLL. The SLL and NDL for the two nulls are given in Table 3. The proposed technique produced a better reduction in SLL and a deeper NDL.

Then we proceeded with null recovery at three different locations. Fig. 5 shows the null recovery at three different locations. The SLL and NDL for three different matching nulls are shown in Table 4. The NDL of all nulls produced by the proposed technique is deeper.

In some cases, we required more nulls to steer in the direction of jammers. In this case, we steered four nulls in the direction of the required jammers. The null steering and SLL reduction are two important

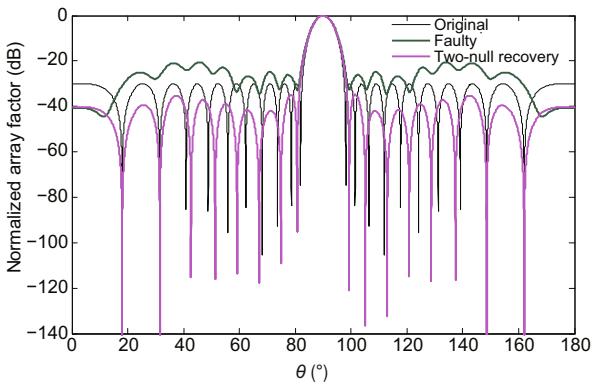

Fig. 4 The original, faulty, and two-null recovered radiation power patterns (References to color refer to the online version of this figure)

Table 3 Comparison of SLL and NDL in the original, faulty, and two-null recovered radiation power patterns

Pattern	Array factor (dB)	
	SLL	NDL
Original	−30.00	−140.00
Damaged	−23.06	−43.98
Recovered	−25.91	−27.57
	−39.40	−140.00
	−35.30	−140.00

SLL: sidelobe level; NDL: null depth level

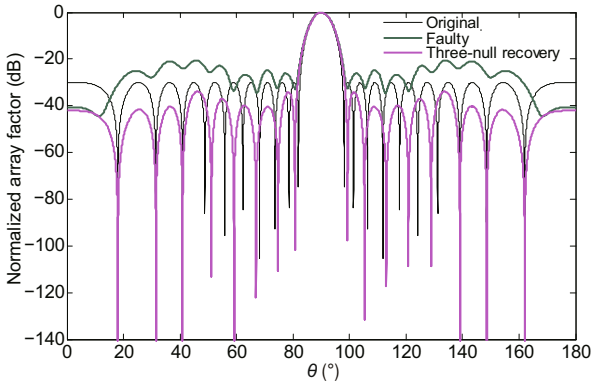

Fig. 5 The original, faulty, and three-null recovered radiation power patterns (References to color refer to the online version of this figure)

issues in failed antenna arrays. To steer nulls to the required locations, we also needed to reduce the corresponding SLL to the desired level. Our proposed technique reduced SLL to the desired level, and produced deeper nulls at the required locations, as shown in Fig. 6. The SLL and NDL for four nulls recovered are shown in Table 5.

Table 4 Comparison of SLL and NDL in the original, faulty, and three-null recovered radiation power patterns

Pattern	Array factor (dB)	
	SLL	NDL
Original	−30.00	−140.00
Damaged	−26.03	−43.98
	−21.71	−27.32
	−21.36	−23.45
Recovered	−41.63	−140.00
	−40.21	−140.00
	−33.86	−140.00

SLL: sidelobe level; NDL: null depth level

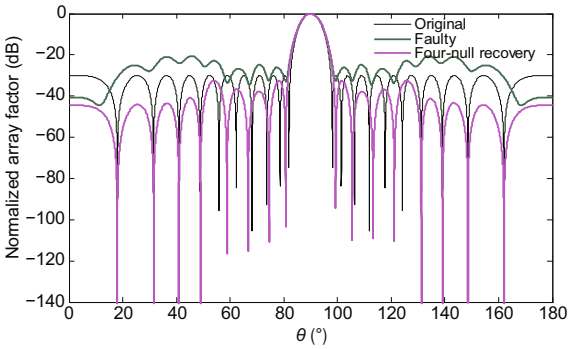

Fig. 6 The original, faulty, and four-null recovered radiation power patterns (References to color refer to the online version of this figure)

Table 5 Comparison of SLL and NDL in the original, faulty, and four-null recovered radiation power patterns

Pattern	Array factor (dB)	
	SLL	NDL
Original	−30.00	−140.00
Damaged	−40.67	−46.32
	−25.24	−27.72
	−21.08	−23.66
	−20.59	−25.69
Recovered	−45.13	−140.00
	−44.14	−140.00
	−44.51	−140.00
	−40.89	−140.00

SLL: sidelobe level; NDL: null depth level

From Fig. 6, it is clear that if we recover more nulls in the desired directions, the radiation power pattern becomes better. In this case, we steered five nulls in the desired directions with a deeper NDL. The proposed technique achieved better SLL, NDL, and null recovery at five different locations, as shown in Fig. 7. The SLL and NDL for five recovered pattern are shown in Table 6.

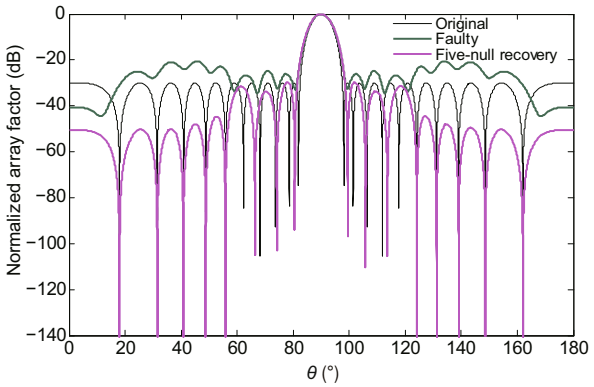

Fig. 7 The original, faulty, and five-null recovered radiation power patterns (References to color refer to the online version of this figure)

Table 6 Comparison of SLL and NDL in the original, faulty, and five-null recovered radiation power patterns

Pattern	Array factor (dB)	
	SLL	NDL
Original	−30.00	−140.00
Damaged	−40.67	−46.32
	−25.24	−27.72
	−21.08	−23.66
	−20.59	−25.69
	−23.17	−32.35
Recovered	−50.53	−140.00
	−50.37	−140.00
	−50.80	−140.00
	−47.95	−140.00
	−44.67	−140.00

SLL: sidelobe level; NDL: null depth level

Because we recovered more nulls in the desired direction, SLL was also reduced to the desired level. The recovery of six nulls with the reduced SLL is shown in Fig. 8. The SLL and NDL achieved by the proposed technique are given in Table 7. The weights obtained by the proposed technique for six recovered nulls are given in Table 8.

4.2 Comparison with conventional techniques

The presentation of the proposed technique is compared with those of conventional techniques (Yeo and Lu, 1999; Khan et al., 2013; Acharya et al., 2014).

Case A: In the first case, the performance of the proposed technique was compared with that of the technique proposed by Yeo and Lu (1999). The parameters of the faulty pattern were distressed in terms

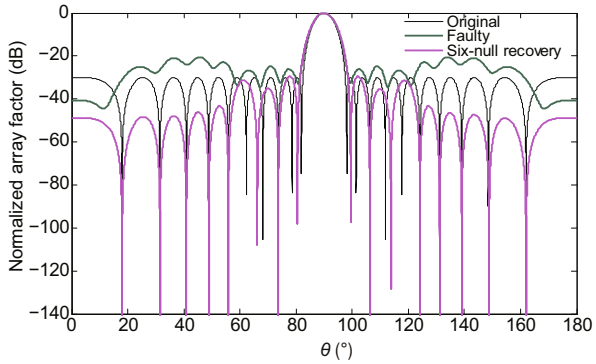

Fig. 8 The original, faulty, and six-null recovered radiation power patterns (References to color refer to the online version of this figure)

of SLL, NDL, dislocation of nulls from their original locations, and main beam width. The objective was to restore SLL to its original pattern by adjusting the weights of the active sensors (Yeo and Lu, 1999); however, the NDL, restoration of the nulls to their original locations, and main beam width were significant issues to be taken into account. Our proposed technique solved the issues of SLL, NDL, restoration of nulls to their original locations, and main beam width. The pattern recovered using the conventional technique is shown in Fig. 9. The SLL and NDL of the technique proposed by Yeo and Lu (1999) and the proposed technique are given in Table 9. The conventional technique (Yeo and Lu, 1999) solved only the SLL issue, while our proposed technique reduced

Table 7 Comparison of SLL and NDL in the original, faulty, and six-null recovered radiation power patterns

Pattern	Array factor (dB)	
	SLL	NDL
Original	−30.00	−140.00
Damaged	−40.67	−46.32
	−25.24	−27.72
	−21.08	−23.66
	−20.59	−25.69
	−23.17	−32.35
	−26.77	−33.89
Recovered	−48.92	−140.00
	−48.44	−140.00
	−48.12	−140.00
	−46.22	−140.00
	−43.20	−140.00
	−35.65	−140.00

SLL: sidelobe level; NDL: null depth level

Table 8 Normalized weights of radiation patterns using different optimization techniques

Element number	Chebyshev weight	Normalized weight			
		Yeo and Lu, 1999	Acharya et al., 2014	Khan et al., 2013	Proposed technique
1	0.3337	0.0361+0.0019i	0.1315	0.0319−0.0008i	0.0798−0.0014i
2	0.2789	0	0	0	0
3	0.3780	0.3409+0.0015i	0.2908	0.1429+0.0005i	0.1160+0.0005i
4	0.4849	0.4266−0.0015i	0.4026	0.4031+0.0001i	0.3809+0.0003i
5	0.5946	0	0	0	0
6	0.7014	0.5404+0.0024i	0.5226	0.5696−0.0004i	0.5845−0.0003i
7	0.7995	0.7006−0.0035i	0.6438	0.6125−0.0002i	0.6545−0.0004i
8	0.8829	0.8007+0.0037i	0.7581	0.7039+0.0007i	0.7214+0.0007i
9	0.9465	0.8818−0.0030i	0.8575	0.8945−0.0002i	0.8643−0.0007i
10	0.9864	0.9466+0.0023i	0.9345	1.0128+0.0002i	0.9775+0.0008i
11	1.0000	0.9876−0.0026i	0.9833	0.9671−0.0007i	0.9765−0.0006i
12	0.9864	0.9982+0.0033i	1.0000	0.9106−0.0000i	0.9498+0.0000i
13	0.9465	0.9878−0.0035i	0.9833	0.9671+0.0007i	0.9765+0.0006i
14	0.8829	0.9454+0.0027i	0.9345	1.0128−0.0002i	0.9775−0.0008i
15	0.7995	0.8846−0.0016i	0.8575	0.8945+0.0002i	0.8643+0.0007i
16	0.7014	0.7966+0.0011i	0.7581	0.7039−0.0007i	0.7214−0.0007i
17	0.5946	0.7050−0.0014i	0.6438	0.6125+0.0002i	0.6545+0.0004i
18	0.4849	0.5913+0.0017i	0.5226	0.5696+0.0004i	0.5845+0.0003i
19	0.3780	0.3756−0.0003i	0.4026	0.4031−0.0001i	0.3809−0.0003i
20	0.2789	0.2819+0.0013i	0.2908	0.1429−0.0005i	0.1160−0.0005i
21	0.3337	0.3300−0.0013i	0.3152	0.0319+0.0008i	0.0798+0.0014i

SLL, achieved a deeper NDL and restoration of the nulls to their original locations.

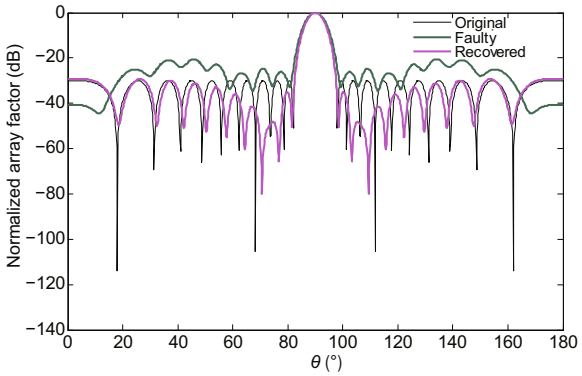

Fig. 9 The original, faulty, and recovered radiation power patterns

The pattern is recovered using the conventional technique proposed by Yeo and Lu (1999). References to color refer to the online version of this figure

Table 9 Comparison of SLL and NDL obtained by the proposed and conventional techniques in recovered radiation power patterns

Technique	Array factor of the recovered nulls (dB)	
	SLL	NDL
Proposed	−48.92	−140.00
	−48.44	−140.00
	−48.12	−140.00
	−46.22	−140.00
	−43.21	−140.00
	−35.65	−140.00
Yeo and Lu, 1999	−47.12	−29.54
	−47.66	−30.01
	−49.51	−31.16
	−51.45	−33.61
	−54.91	−36.31
	−57.75	−41.46
Acharya et al., 2014	−31.68	−32.73
	−31.14	−33.35
	−30.59	−33.47
	−29.94	−34.55
	−29.31	−36.54
	−28.52	−37.95
Khan et al., 2013	−40.38	−116.10
	−40.08	−105.80
	−41.40	−101.40
	−49.33	−100.20
	−35.72	−96.48
	−27.75	−96.80

SLL: sidelobe level; NDL: null depth level

If antenna sensors fail and users vary their locations, then we can steer the main beam in the direction of target users. In this case, the main beam was pointing at an angle of 60° with nulls restored to their particular locations (Fig. 10).

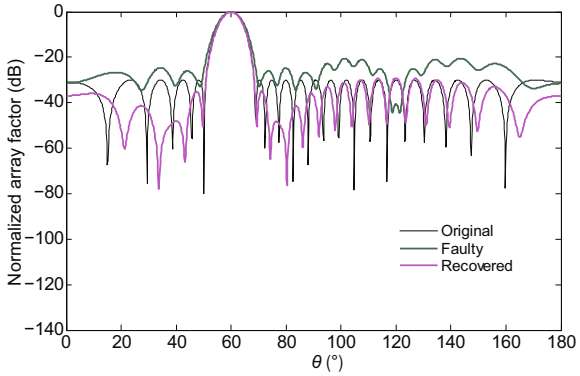

Fig. 10 The original, faulty, and main beam recovered patterns pointing at 60°

The pattern is recovered using the conventional technique proposed by Yeo and Lu (1999). References to color refer to the online version of this figure

If the desired users change their positions to other locations, we will steer the main beam in that particular direction. In Fig. 11, the main beam is steered in the direction of 120°. The weights obtained using the conventional technique proposed by Yeo and Lu (1999) for the main beam steered at 120° are given in Table 8.

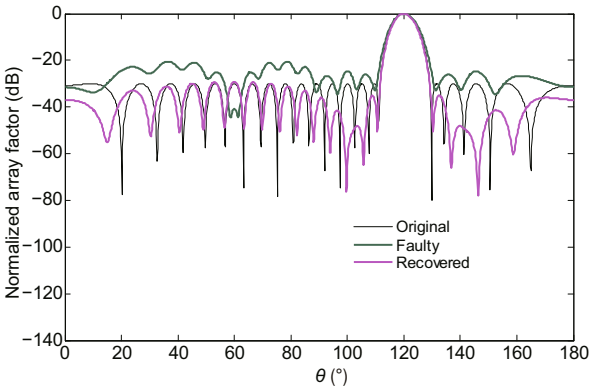

Fig. 11 The original, faulty, and main beam recovered patterns pointing at 120°

The pattern is recovered using the conventional technique proposed by Yeo and Lu (1999). References to color refer to the online version of this figure

Case B: In this case, the performance of the proposed technique was compared with that of the technique proposed by Acharya et al. (2014). This conventional technique recovered only SLL by readjusting the weights of the active sensors, while again, NDL, restoration of the nulls to their original locations, and main beam width were still issues to be considered. After optimization by the proposed technique, we obtained a better pattern in terms of SLL, NDL, restoration of nulls to their original locations, and main beam width. Figs. 12–14 show the different patterns recovered using the conventional technique proposed by Acharya et al. (2014), which recovered only SLL. The SLL and NDL parameters for the technique proposed by Acharya et al. (2014) and the proposed technique are given in Table 8. The main beam recovered using the conventional technique (Acharya et al., 2014) pointed at an angle of θ_s=120° is shown in Fig. 15. The weights of the recovered pattern obtained by the conventional technique (Acharya et al., 2014) for the main beam pointed at 120° are given in Table 8.

Case C: In this case, the performance of the proposed technique was compared with that of the conventional technique proposed by Khan et al. (2013). In this conventional technique, NDL, restoration of nulls to their original locations, and main beam width were achieved; however, SLL was higher, especially at the first three peaks near the main beam. Our proposed technique resolved all the issues, and obtained a deeper NDL and a reduced SLL (Fig. 16). This is very important in signal processing. The SLL and NDL for this conventional technique (Khan et al., 2013) and the proposed technique are given in Table 9. The weights recovered using the conventional technique (Khan et al., 2013) for recovery of six nulls are given in Table 8.

Case D: In this case, we assumed the failure of four sensors, i.e., w_2, w_3, w_4, and w_5, which caused the pattern to be disturbed badly as shown in Fig. 17. In the corrected pattern, SLL and nulls in their original positions were recovered; however, we received a broader main beam width. From the results of this simulation, it is clear that if more sensors become faulty, the main beam width will be broader.

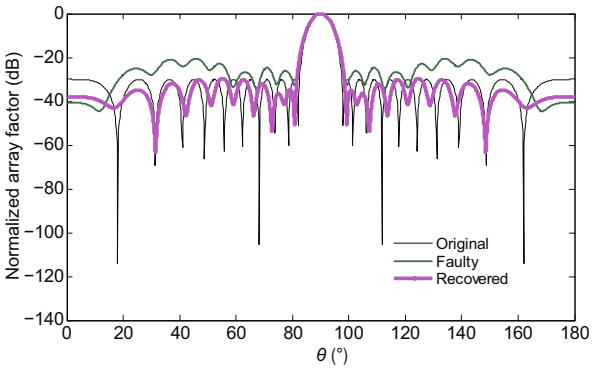

Fig. 12 The original, faulty, and ripple sidelobe recovered patterns

The pattern is recovered using the conventional technique proposed by Acharya et al. (2014). References to color refer to the online version of this figure

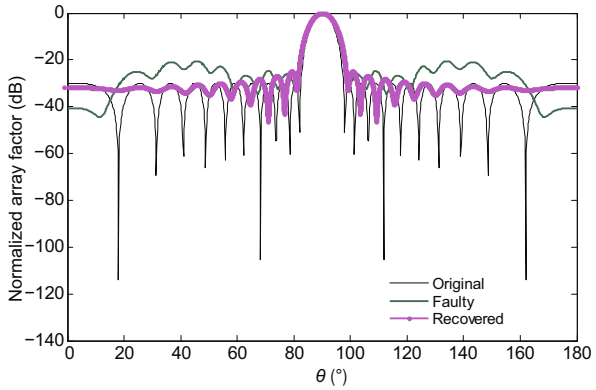

Fig. 13 The original, faulty, and flat sidelobe recovered patterns

The pattern is recovered using the conventional technique proposed by Acharya et al. (2014). References to color refer to the online version of this figure

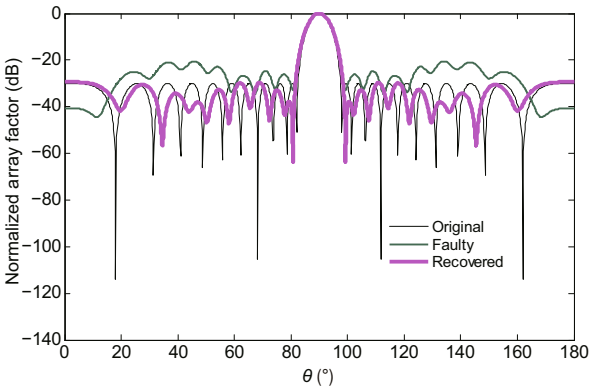

Fig. 14 The original, faulty, and sidelobe along with null recovered patterns

The pattern is recovered using the conventional technique proposed by Acharya et al. (2014). References to color refer to the online version of this figure

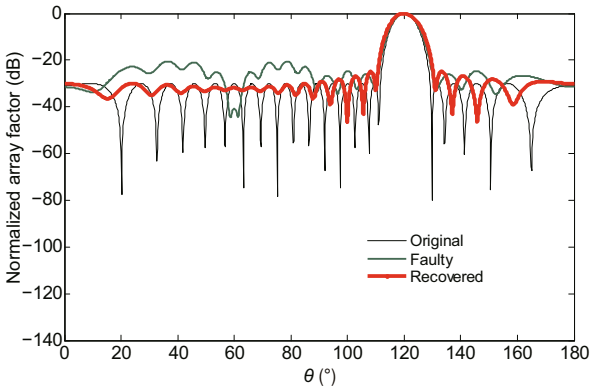

Fig. 15 The original, faulty, and main beam recovered patterns pointing at 120°

The pattern is recovered using the conventional technique proposed by Acharya et al. (2014). References to color refer to the online version of this figure

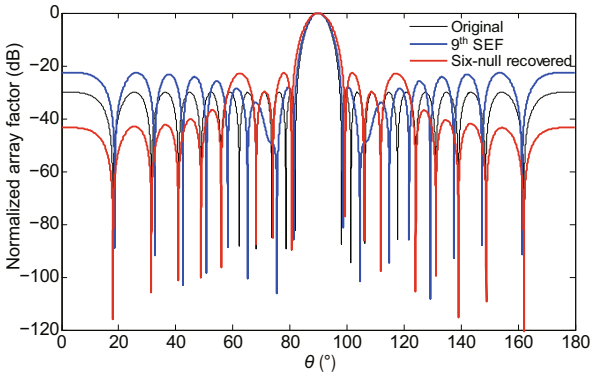

Fig. 16 The original, the 9th symmetrical element failure (SEF), and six-null recovered radiation power patterns

The pattern is recovered using the conventional technique proposed by Khan et al. (2013). References to color refer to the online version of this figure

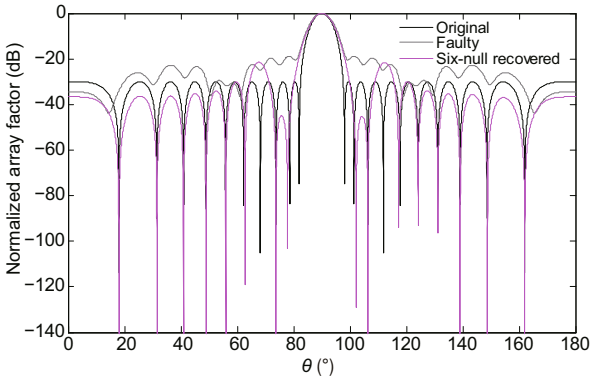

Fig. 17 The original, four-element faulty, and six-null recovered patterns (References to color refer to the online version of this figure)

5 Conclusions and future work

The proposed fitness function corrects the damaged patterns in terms of SLL, NDL, and restoration of nulls to their desired locations using the nature-inspired GWO hybridized with an IPA. The fitness function consists of three factors, which are necessary for failure correction, and the proper fittings of the parameters in the fitness function give the desired pattern. The hybrid algorithm gives better results than the existing algorithms in terms of sidelobes, null depth, and placement of nulls at the desired locations. The numerical simulation showed that a better pattern can be achieved with the proposed hybrid algorithm. This method can be extended to circular arrays.

References

Acharya OP, Patnaik A, Sinha SN, 2011. Null steering in failed antenna arrays. *Appl Comput Intell Soft Comput*, 2011: 692197. https://doi.org/10.1155/2011/692197

Acharya OP, Patnaik A, Sinha SN, 2014. Limits of compensation in a failed antenna array. *Int J RF Microw Comput Aided Eng*, 24(6):635-645. https://doi.org/10.1002/mmce.20807

Choudhury B, Acharya OP, Patnaik A, 2013. Bacteria foraging optimization in antenna engineering: an application to array fault finding. *Int J RF Microw Comput Aided Eng*, 23(2):141-148. https://doi.org/10.1002/mmce.20659

El-Gaafary AAM, Mohamed YS, Hemeida AM, et al., 2015. Grey wolf optimization for multi input multi output system. *Univ J Commun Netw*, 3(1):1-6. https://doi.org/10.13189/ujcn.2015.030101

Fonollosa J, Vergara A, Huerta R, 2013. Algorithmic mitigation of sensor failure: is sensor replacement really necessary? *Sens Actuat B*, 183:211-221. https://doi.org/10.1016/j.snb.2013.03.034

Hejres JA, 2004. Null steering in phased arrays by controlling the positions of selected elements. *IEEE Trans Antennas Propag*, 52(11):2891-2895. https://doi.org/10.1109/TAP.2004.835128

Hejres JA, Peng A, Hijres J, 2007. Fast method for sidelobe nulling in a partially adaptive linear array using the elements positions. *IEEE Antennas Wirel Propag Lett*, 6:332-335. https://doi.org/10.1109/LAWP.2007.900955

Khan SU, Qureshi IM, Zaman F, et al., 2013. Null placement and sidelobe suppression in failed array using symmetrical element failure technique and hybrid heuristic computation. *Prog Electromag Res B*, 52:165-184. https://doi.org/10.2528/PIERB13032712

Khan SU, Qureshi IM, Zaman F, et al., 2014. Correction of faulty sensors in phased array radars using symmetrical sensor failure technique and cultural algorithm with dif-

ferential evolution. *Sci World J*, 2014:852539. https://doi.org/10.1155/2014/852539

Khan SU, Qureshi IM, Zaman F, et al., 2015a. An application of hybrid nature inspired computational technique to detect faulty element in array antenna. Proc 12th Int Bhurban Conf on Applied Sciences and Technology, p.629-632. https://doi.org/10.1109/IBCAST.2015.7058572

Khan SU, Qureshi IM, Shoaib B, et al., 2015b. Correction of faulty pattern using cuckoo search algorithm and symmetrical element failure technique along with distance adjustment between the antenna array. Proc 12th Int Bhurban Conf on Applied Sciences and Technology, p.633-636. https://doi.org/10.1109/IBCAST.2015.7058573

Khan SU, Qureshi IM, Shoaib B, 2015c. Meta-heuristic cuckoo search algorithm for the correction of failed array antenna. *Mehran Univ Res J*, 34(4):325-336.

Khan SU, Qureshi IM, Naveed A, et al., 2016a. Detection of defective sensors in phased array using compressed sensing and hybrid genetic algorithm. *J Sens*, 2016: 6139802. https://doi.org/10.1155/2016/6139802

Khan SU, Qureshi IM, Haider H, et al., 2016b. Diagnosis of faulty sensors in phased array radar using compressed sensing and hybrid IRLS-SSF algorithm. *Wirel Pers Commun*, 91(2):383-402. https://doi.org/10.1007/s11277-016-3466-7

Khan SU, Qureshi IM, Shoaib B, et al., 2016c. Recovery of failed element signal with a digitally beamforming using linear symmetrical array antenna. *J Inform Sci Eng*, 32(3): 611-624.

Khan SU, Qureshi IM, Zaman F, et al., 2017. Detecting faulty sensors in an array using symmetrical structure and cultural algorithm hybridized with differential evolution. *Front Inform Technol Electron Eng*, 18(2):235-245. https://doi.org/10.1631/FITEE.1500315

Mirjalili S, Mirjalili SM, Lewis A, 2014. Grey wolf optimizer. *Adv Eng Softw*, 69:46-61. https://doi.org/10.1016/j.advengsoft.2013.12.007

Muro C, Escobedo R, Spector L, et al., 2011. Wolf-pack (*Canis lupus*) hunting strategies emerge from simple rules in computational simulations. *Behav Process*, 88(3):192-197. https://doi.org/10.1016/j.beproc.2011.09.006

Peters TJ, 1991. A conjugate gradient-based algorithm to minimize the sidelobe level of planar arrays with element failures. *IEEE Trans Antennas Propag*, 39(10):1497-1504. https://doi.org/10.1109/8.97381

Poli L, Rocca P, Oliveri G, et al., 2014. Failure correction in time-modulated linear arrays. *IET Radar Sonar Navig*, 8(3):195-201. https://doi.org/10.1049/iet-rsn.2013.0027

Potra FA, Wright SJ, 2000. Interior-point methods. *J Comput Appl Math*, 124(1-2):281-302. https://doi.org/10.1016/S0377-0427(00)00433-7

Raja MAZ, Ahmad I, Khan I, et al., 2017. Neuro-heuristic computational intelligence for solving nonlinear pantograph systems. *Front Inform Technol Electron Eng*, 18(4): 464-484. https://doi.org/10.1631/FITEE.1500393

Ram G, Mandal D, Ghoshal SP, et al., 2017. Optimal array factor radiation pattern synthesis for linear antenna array using cat swarm optimization: validation by an electromagnetic simulator. *Front Inform Technol Electron Eng*, 18(4):570-577. https://doi.org/10.1631/FITEE.1500371

Shoaib B, Qureshi IM, Butt SA, et al., 2015. Adaptive step size kernel least mean square algorithm for Lorenz time series prediction. Proc 12th Int Bhurban Conf on Applied Sciences and Technology, p.218-221. https://doi.org/10.1109/IBCAST.2015.7058507

Song HM, Sulaiman MH, Mohamed MR, 2014. An application of grey wolf optimizer for solving combined economic emission dispatch problems. *Int Rev Model Simul*, 7(5): 838-844. https://doi.org/10.15866/iremos.v7i5.2799

Uysal A, Bayir R, 2013. Real-time condition monitoring and-fault diagnosis in switched reluctance motors with Kohonen neural network. *J Zhejiang Univ-Sci C (Comput & Electron)*, 14(12):941-952. https://doi.org/10.1631/jzus.C1300085

Wolff I, 1937. Determination of the radiating system which will produce a specified directional characteristic. *Proc Inst Radio Eng*, 25(5):630-643. https://doi.org/10.1109/JRPROC.1937.228158

Wong LI, Sulaiman MH, Mohamed MR, et al., 2014. Grey wolf optimizer for solving economic dispatch problems. Proc IEEE Int Conf on Power and Energy, p.150-154. https://doi.org/10.1109/PECON.2014.7062431

Wright SJ, 1997. Primal-Dual Interior-Point Methods. Society for Industrial and Applied Mathematics, Philadelphia, USA.

Yeo BK, Lu YL, 1999. Array failure correction with a genetic algorithm. *IEEE Trans Antennas Propag*, 47(5):823-828. https://doi.org/10.1109/8.774136

Zhang HW, Xie JW, Lu WL, et al., 2017. A scheduling method based on a hybrid genetic particle swarm algorithm for multifunction phased array radar. *Front Inform Technol Electron Eng*, 18(11):1806-1816. https://doi.org/10.1631/FITEE.1601358

Zhu CL, Wang WQ, Chen H, et al., 2015. Impaired sensor diagnosis, beamforming, and DOA estimation with difference co-array processing. *IEEE Sens J*, 15(7):3773-3780. https://doi.org/10.1109/JSEN.2015.2399510

Zou DX, Wang GG, Pan G, et al., 2016. A modified simulated annealing algorithm and an excessive area model for floorplanning using fixed-outline constraints. *Front Inform Technol Electron Eng*, 17(11):1228-1244. https://doi.org/10.1631/FITEE.1500386